RSC Advances

ROYAL SOCIETY OF CHEMISTRY

www.rsc.org/advances

Graphical abstract

Water dispersible, β-cyclodextrin functionalized, magnetite nanoparticles are shown to be suitable for the delivery of the hydrophobic drug curcumin, with possible multifunctional applications.

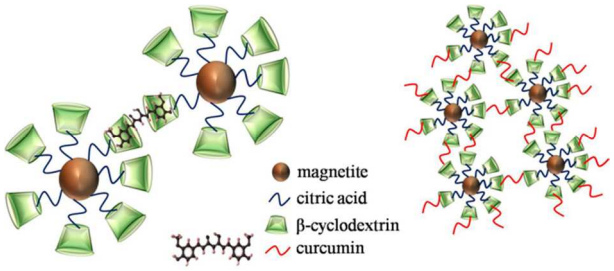

Citrate modified β-cyclodextrin functionalized magnetite nanoparticles: A biocompatible platform for hydrophobic drug delivery

Kunnoth N. Jayaprabha and Pattayil A. Joy*

Physical and Materials Chemistry Division, CSIR-National Chemical laboratory

Pune, India, 411008

E-mail: pa.joy@ncl.res.in

Abstract

Water-dispersible magnetite nanoparticles functionalized with citric acid (CIT) modified β-cyclodextrin (CD) are prepared and curcumin (CUR) is loaded inside the cavity of CD. The CUR loading capacity of CD-CIT functionalized magnetite nanoparticles is found to be much larger than that of CD alone as well as the CD-CIT conjugate. The release profile of curcumin is found to follow zero order kinetics at the physiological pH, and thus, can release CUR at a constant rate, after the initial burst release. Relaxivity studies using NMR showed that the functionalized nanoparticles are suitable for contrast enhancement in MRI. Thus, the water-dispersible, CIT modified β-CD functionalized magnetite nanofluid is an efficient carrier for water insoluble curcumin, and can be used for magnetic drug targeting/delivery as well as for contrast enhancement in MRI due to the superparamagnetic magnetite core.

Keywords: Water dispersible nanoparticles; Superparamagnetic nanoparticles; Hydrophobic drug loading; Curcumin; Cyclodextrin; Drug delivery; MRI

I. Introduction

Drug targeting and release, especially hydrophobic drugs, is an area of intense research using nanomaterials with an emphasis on their multifunctionality. Continuous efforts are being made to develop systems for controlled release of drugs because the appropriate dosage decides the therapeutic efficiency of the drugs. The main objectives of the current drug delivery research using appropriate nanoparticles are to develop specific targeting and delivery of drugs, reduction in toxicity while maintaining the therapeutic effects, greater safety and biocompatibility.[1]Drug delivery systems being developed based on nanotechnology include polymeric micelles, polymeric nanoparticles, magnetic nanoparticles, liposomes and dendrimers.[2-4] Of all these, magnetic nanoparticles are of specific interest in drug delivery due to the benefit of targeting the carrier using an external magnetic field,[5] and therefore, the use of magnetic nanoparticles for site-specific drug release are also an important area of research.[6] Nanoparticles with magnetite core and organic surface coating are being developed for theragnostic applications, which can be simultaneously used for imaging, targeting and drug delivery.[7]

Superparamagnetic iron oxide nanoparticles (SPIONs) have gained the attention of researchers due to their biocompatibility and unique magnetic properties at the nanoregime where these nanoparticles exhibit magnetism only in the presence of a magnetic field.[8] Modified SPIONs are widely marketed as MRI contrast agents in different names such as ferridex, ferrumoxtran, resovist, *etc.*[9] Iron oxide (Fe_3O_4, magnetite) nanoparticles coated with suitable molecules also act as a multifunctional platform which can be simultaneously used as contrast agents in magnetic resonance imaging (MRI), magnetic hyperthermia and drug delivery.[10] Even though magnetite nanoparticles are studied during the past many decades, stabilization of these nanoparticles in aqueous medium is still a challenge. The nanoparticles undergo aggregation by van der Waal's interaction, apart from the aggregation due to the magnetic dipole-dipole interactions.[11] Hence, it is necessary to coat the surface of the magnetite nanoparticles with suitable surfactants to avoid aggregation and the coated nanoparticles should be biocompatible and biodegradable to be used for biomedical applications.[12]

Even though there are various reports on the biomedical applications of magnetite nanoparticles, delivery of hydrophobic drugs using these particles, without losing the therapeutic efficacy of the drug is of great importance. The delivery of the hydrophobic drugs to the target

site is suggested through different carriers like polymeric micelles, silica nanoparticles, cyclodextrin derivatives *etc.*[13-15] Of these, cyclodextrins, which have a hydrophobic cavity, can be an efficient candidate for entrapment of hydrophobic drugs. Cyclodextrins are cyclic oligosaccharides of a glucopyranose, with a hydrophobic inner cavity and hydrophilic outer surface.[16] These molecules easily form inclusion complexes both in solution and solid state.[17] The widely used natural cyclodextrins areα-, β-, and γ-cyclodextrins, consisting of six, seven, and eight D-glucopyranose residues, respectively, linked by α-1,4 glycosidic bonds into a macrocycle. They are known to have the ability to form inclusion complexes with guest molecules, which is being widely applied in food, cosmetics and pharmaceutical industries and also for analytical purpose. β-cyclodextrin, the most common natural cyclodextrin, has 21 hydroxyl groups with a cavity diameter of 7.8Å.[18] It is also used as a drug carrier to increase the stability, solubility and bioavailability of drug molecules.[19]

Curcumin is well-known for its anti-cancer activity and there is a renewed interest in the recent past on the studies on the delivery of curcumin at the target site using a carrier, due to its poor water solubility.[20,21,22] Citric acid modified β-cyclodextrin is reported to be an efficient carrier of water insoluble drugs,[23] and cyclodextrin derivative has been studied for the delivery of potential anti-cancer agents like curcumin.[24] Cyclodextrin forms a stable inclusion complex with curcumin by supramolecular host-guest interaction[25] and the inner cavity of the beta form is more appropriate for curcumin loading than the α and γ forms.[26] The use of magnetite nanoparticles with a cyclodextrin shell can play a multifunctional role in biomedical applications.[27] Water based magnetic fluids, functionalized with cyclodextrin, can be an efficient carrier for hydrophobic drugs and therefore can be used for delivery of the water insoluble drugs at specific sites. The presence of the superparamagnetic magnetite core makes them efficient candidates to be used as a negative contrast agent in magnetic resonance imaging (MRI). Here we report the synthesis, characterization, and studies on curcumin loaded, citric acid modified β-cyclodextrin (CD) capped magnetite nanoparticles. CD has been treated with citric acid (CIT) to form a CD-citric acid conjugate (CD-CIT) to increase the water solubility of CD. It is found that the curcumin loading capacity of CD is increased after functionalizing on the nanoparticles. Thus, the magnetic core and the cyclodextrin coating make the water dispersible fluid an efficient platform for simultaneous imaging (by MRI), drug targeting and delivery.

II. Experimental

Materials: Ferric chloride hexahydrate (≥98%), ferrous chloride tetrahydrate (99%), citric acid monohydrate, curcumin and β-cyclodextrin were purchased from Sigma Aldrich. Ammonium hydroxide (25%), dimethyl sulphoxide (DMSO), nitric acid and 2-propanol were procured from Merck. All the chemicals were used without further purification and double distilled water was used throughout this work.

Preparation of CD-CIT complex: The CD-CIT complex was prepared by modifying the procedure reported by El-Tahlawy *et al.*[28] 3 g of β-cyclodextrin and 1 g of citric acid was dissolved in 10 ml of water and the mixture was stirred at 80 ^{o}C for three hours. The transparent solution obtained was treated with 2-propanol, which gave a white precipitate. The product was washed thoroughly to remove unreacted components and further dried at 60 ^{o}C for 24 hours to get the white CD-CIT complex.

Preparation of surface functionalized magnetite nanoparticles: Magnetite nanoparticles were prepared by the reverse co-precipitation method.[29] A mixed solution of 2 mmol of $FeCl_3.6H_2O$ and 1 mmol of $FeCl_2.4H_2O$ in water was added to 100 ml of 19% ammonium hydroxide solution under argon atmosphere. The mixture was stirred well for complete formation and growth of magnetite nanoparticles. The nanoparticles were washed with distilled water to remove excess base. Then the pH was brought down to 7 by washing with water and the resultant nanoparticles were re-dispersed in 100 ml distilled water. 2 g of the CD-CIT complex dissolved in water was added drop-wise to the dispersion and stirred for 4 hours at 80 ^{o}C. The stable dispersion obtained was then dialyzed against water for three days to remove excess CD-CIT complex. The dispersion was then dried at 70 ^{o}C to get solid nanoparticles. The coated nanoparticles were well dispersible in water and at the physiological pH to form a nanofluid. The sample was labeled as CDmf. Citric acid coated magnetite nanoparticles were also synthesized following the same procedure for comparison. The nanoparticles coated with citric acid also formed stable dispersion in aqueous media and was labeled as CITmf. Uncoated nanoparticles were also prepared under the same reaction conditions and labeled as Unmf.

Magnetite nanoparticles directly coated with curcumin was synthesized by the procedure reported earlier.[30] Briefly, a mixture of ferric chloride hexahydrate and ferrous chloride

tetrahydrate, taken in the molar ratio of 2:1, was added to ammonia solution to form magnetite nanoparticles. After stirring for 30 minutes, dilute nitric acid was added to bring down the pH to ~8-9. Curcumin solution at the same pH was added and the dispersion was stirred for the effective coating of curcumin to magnetite nanoparticles. The final dispersion was dialyzed against water to remove unreacted excess curcumin and ammonia. The dispersion was dried to get a powder which forms stable dispersion in dimethyl sulfoxide. The curcumin encapsulated sample was labeled as CURmf.

Preparation of CUR inclusion complex: The inclusion complexes were prepared by modifying the procedure reported by Yallappu *et al.*[31] 20 mg of the CD-CIT coated sample (CDmf) was dispersed in 30 ml water in a 50 ml vial. To this dispersion, varying amounts of curcumin (10 mg, 20 mg and 30 mg), dissolved in 1 ml acetone, were added while stirring gently. The mixture was stirred for 6 hours to evaporate acetone. The dispersion was then stirred overnight and centrifuged at 5000 rpm for 5 minutes. The supernatant liquid which contains highly water dispersed inclusion complex was dried and stored at 5 ^{o}C for further use. The resultant inclusion complexes were labeled as CDmf10, CDmf20 and CDmf30. Inclusion complexes were also prepared using CD alone and the CD-CIT conjugate using 20 mg curcumin and 20 mg of the compound. They were designated as CD20 and CD-CIT20, respectively.

Curcumin loading studies: 1mg of the solid curcumin inclusion complex was dispersed in 10 ml dimethyl sulfoxide (DMSO) to extract the curcumin to the solvent. This dispersion was shaken on a vortex shaker for 24 hours at room temperature. The vial containing the dispersion was covered with an aluminium foil to prevent exposure to light. The dispersion was then centrifuged at 10000 rpm to remove the curcumin-free CD-CIT coated sample and the clear yellow supernatant solution of curcumin in DMSO was collected and used for estimation. The amount of curcumin released was estimated from the absorbance measured at 425 nm using a standard graph of absorbance of curcumin dissolved in DMSO.

The curcumin entrapment efficiency (EE) is calculated using the formula:

$$EE(\%) = \frac{mass\ of\ curcumin\ trapped}{mass\ of\ curcumin\ used} \text{ x } 100$$

In vitro release: The release of curcumin from the CD-CIT coated sample was done at pH 7.4 and pH 5.5, by the dialysis bag method. The CDmf20 sample which showed maximum curcumin loading was dispersed in the phosphate buffer (pH = 7.4) at a concentration of 1 mg/ml, sonicated to form a stable dispersion and was transferred to a dialysis bag. The dialysis bag tied at both ends was immersed in 50 ml buffer solution and stirred gently. 2 ml of the buffer was withdrawn at particular intervals and replenished with the same amount of fresh buffer. The absorbance was measured at 425 nm, the λ_{max} for curcumin. The amount of curcumin released was then plotted against time. Release rate of curcumin was also determined using acetate buffer (pH = 5.5) using the same procedure.

Characterization: Phase purity of the iron oxide nanoparticles was determined by powder X-ray diffraction (XRD) using a PANalytical X'PERT PRO model X-ray diffractometer, in the 2θ range of 10 to 80 degrees, using Cu Kα radiation. TEM analysis was performed on a FEI, TECNAI G2 TF30 instrument. Samples were prepared by placing a drop of dilute dispersion on a carbon coated 200 mesh copper grid and imaged at an accelerating voltage of 300kV. Zeta potential and hydrodynamic particle size were measured using the dynamic light scattering (DLS) technique using a Brookhaven instruments 90Plus Particle Size Analyzer equipped with a 632.8 nm laser. Infrared spectra were recorded on a Tensor 27 Bruker FT-IR spectrometer, using KBr pellets, in the frequency range of 4000–400 cm^{-1}. Thermogravimetric analysis (TGA) of the synthesized samples, in air, was performed on a Perkin-Elmer TGA7 analyzer. Magnetic measurements were carried out on a Quantum Design MPMS 7TSQUID-VSM. Zero field cooled (ZFC) and field cooled (FC) magnetization measurements were carried out in an applied field of 5 mT (50 Oe) and magnetization versus field measurements, at room temperature, were carried out from −3 T to +3 T. UV-Visible spectra were recorded using a Cary 5000 UV-Vis-NIR spectrophotometer and the measurements were carried out in a Quartz cell of 10mm path length. The absorbance measurements for the study of curcumin release were also done on the same instrument. Fluorescence measurements were performed using a Photon Technology International fluorescence QM40 spectrophotometer with a Quartz cell of 10 mm path length. The T_1 and T_2 relaxation studies were done on a Bruker AV400 NMR spectrometer at a magnetic field of 9.4 Tesla and 400 MHz frequency.

III. Results and Discussion

Table 1: Sample codes/labels used and their description

Sample label	Description
CIT	Citric acid
CD	β-Cyclodextrin
CUR	Curcumin
CD-CIT	Cyclodextrin-citrate complex
Unmf	Uncoated magnetite nanoparticles
CITmf	Citric acid coated magnetite nanoparticles/nanofluids
CURmf	Curcumin coated magnetite nanoparticles/nanofluids
CDmf	CD-CIT coated magnetite nanoparticles/nanofluids
CDmf10, CDmf20, CDmf30	Curcumin loaded CDmf nanofluids by using 20 mg of CDmf and 10, 20 and 30 mg of curcumin, respectively
CD20	Curcumin loaded CD using 20 mg of curcumin
CD-CIT20	Curcumin loaded CD-CIT using 20 mg of curcumin

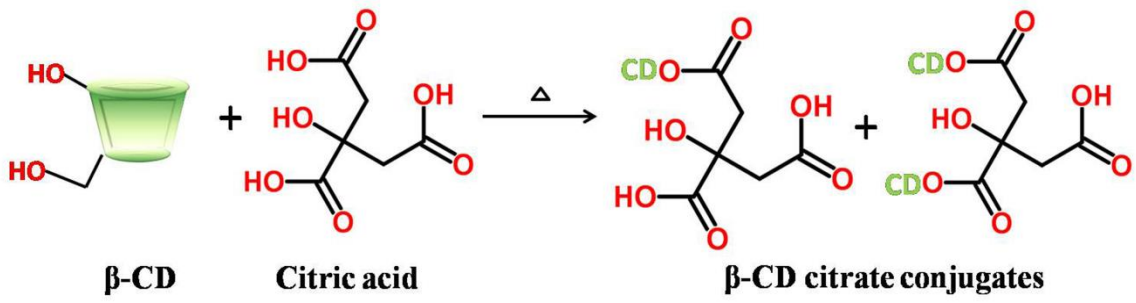

Scheme 1: Reaction between β-cyclodextrin (CD) and citric acid to form the ester. β-cyclodextrin is a truncated cone-shaped molecule with secondary hydroxyl groups on the larger rim and the primary hydroxyl groups on the smaller rim.

Water soluble CD-CIT complex is formed by the esterification between the primary hydroxyl group of CD and the -COOH group of citric acid. The possible products after the reaction are shown in Scheme1. Evidence for the formation of the CD-CIT complex as well as information on the effectiveness of coating of the CD-CIT conjugate on the surface of the magnetite nanoparticles is confirmed from infrared spectroscopic studies. The IR spectra of CD, citric acid, CD-CIT complex and CDmf20 are shown in Fig. 1. The spectra of the CD-CIT complex resemble the spectra of CD. The major bands at 3350 cm^{-1}, 2925 cm^{-1}, 1158 cm^{-1} and 1029 cm^{-1} of CD correspond to the stretching vibrations of -OH, -CH_2, -C-C and bending

vibration of –OH groups, respectively. The band at 1645 cm^{-1} corresponds to the H-O-H deformation band of water present in the cavity of CD. The band at 1750 cm^{-1} in the spectra of citric acid is due to the vibration of the C=O group of the carboxylic acid and this band is shifted to 1730 cm^{-1} in CD-CIT due to the formation of ester.[28] The band at 1730 cm^{-1}, which is due to the C=O stretching of the ester group, is a clear indication for the formation of the CD-CIT conjugate. The intensity of this band of CD-CIT is reduced in CDmf, after coating on the magnetite nanoparticles, indicating that the CD-CIT conjugate binds to the nanoparticle via the C=O group of the citric acid. The bands in the IR spectra of the coated nanoparticles resemble that of the CD-CIT conjugate indicating the bonding of the conjugate to nanoparticles surface. The band at 1645 cm^{-1} corresponding to the vibrations of water in the CD cavity is found to be retained in the coated nanoparticles also, indicating that the iron oxide nanoparticles are not occupied inside the cavity and binds to the CD-CIT complex without disturbing the cavity.[32,33]

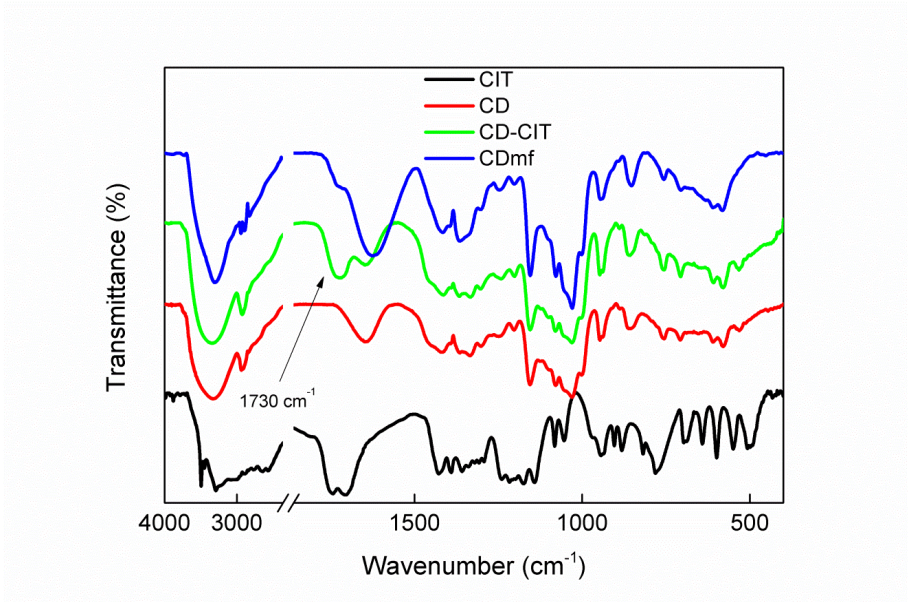

Fig. 1 IR spectra of citric acid (CIT), citric acid-cyclodextrin complex (CD-CIT), β-cyclodextrin (CD), citric acid (CIT) and the CD-CIT coated magnetite nanoparticles (CDmf).

The average crystallite size of the CDmf nanoparticles is calculated as 5 nm from the XRD pattern using the Scherrer equation.[34] The TEM image in Fig. 2(a) shows isolated particles with average particle size of 5 nm, comparable to the crystallite size. Average particle size of 7.7 nm, with a polydispersity of 0.261, is obtained from DLS measurements as shown in Fig. 2(b).

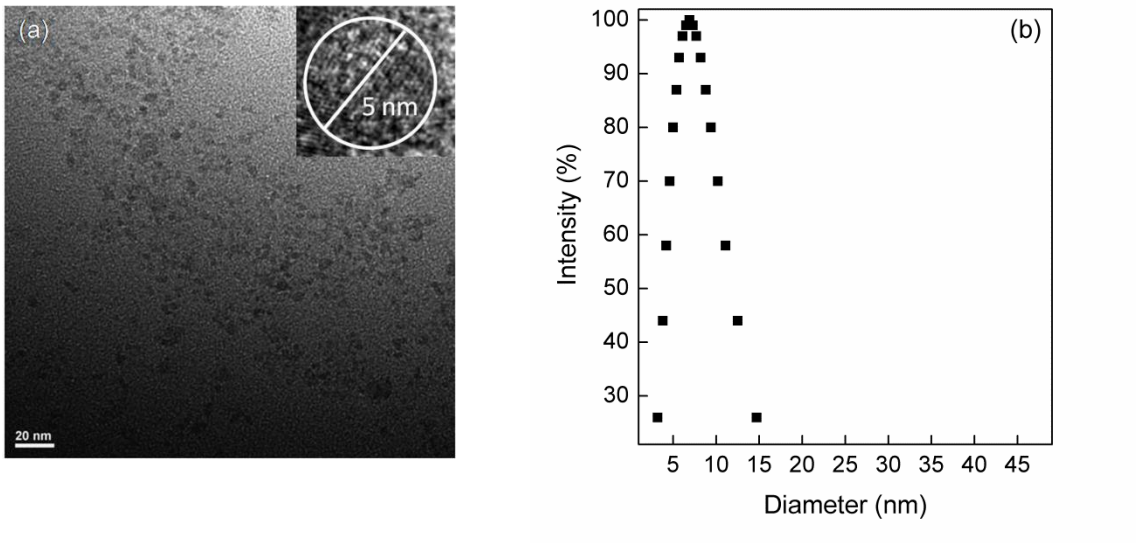

Fig. 2 (a) TEM image of CDmf with the inset showing a single particle of size 5 nm, and (b) the log-normal size distribution from DLS measurement showing a mean particle size of 7.7 nm.

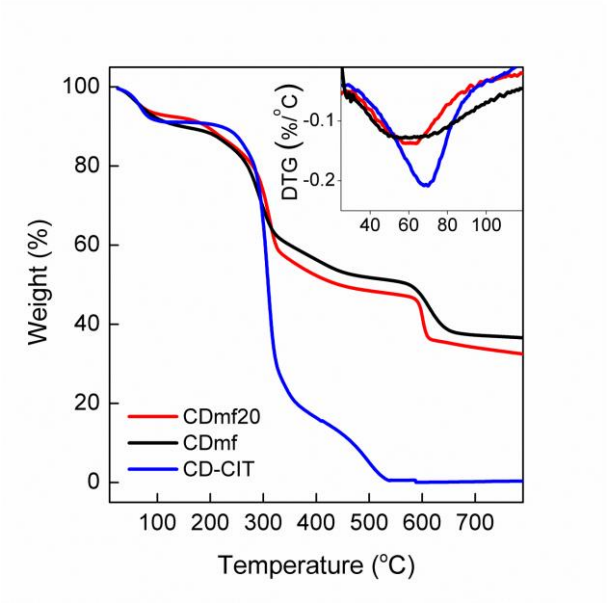

Fig. 3 TGA curves of the CD-CIT complex, CDmf and curcumin loaded CDmf (CDmf20). The inset shows the corresponding differential thermograms (DTG).

TGA curve of CDmf is compared with that of CD and the CD-CIT conjugate in Fig. 3. The total weight loss for CDmf is about 60% and the weight loss path resembles that of bare CD-CIT conjugate, except for a shift in the third weight loss to higher temperatures. The differential

thermograms (DTG) of both curcumin treated and untreated sample are used to calculate the amount of water expelled from the cavity of CD (host) to accommodate the curcumin molecule (guest). Dehydration of CDmf and CD-CIT caused a total mass loss of 8.2% and 8.5% (first weight loss below 100 ^{o}C), and this corresponds to loss of 6.3 and 6.1 water molecules, respectively, from the cavity of CD. The dehydration of CDmf20 results in a mass loss of 6.1%, indicating the removal of 4.5 water molecules from the CD cavity. Thus, the TGA/DTG results indicate that a fraction of the water molecules has escaped from the CD cavity to accommodate the guest molecule (CUR).It is known that, in aqueous solution, the slightly apolar cyclodextrin cavity is occupied by water molecules which are energetically unfavored (polar-apolar interaction), and therefore can be readily substituted by appropriate guest molecules which are less polar than water. The driving force for the complex formation is the substitution of the high enthalpy water molecules by an appropriate guest molecule.[35]

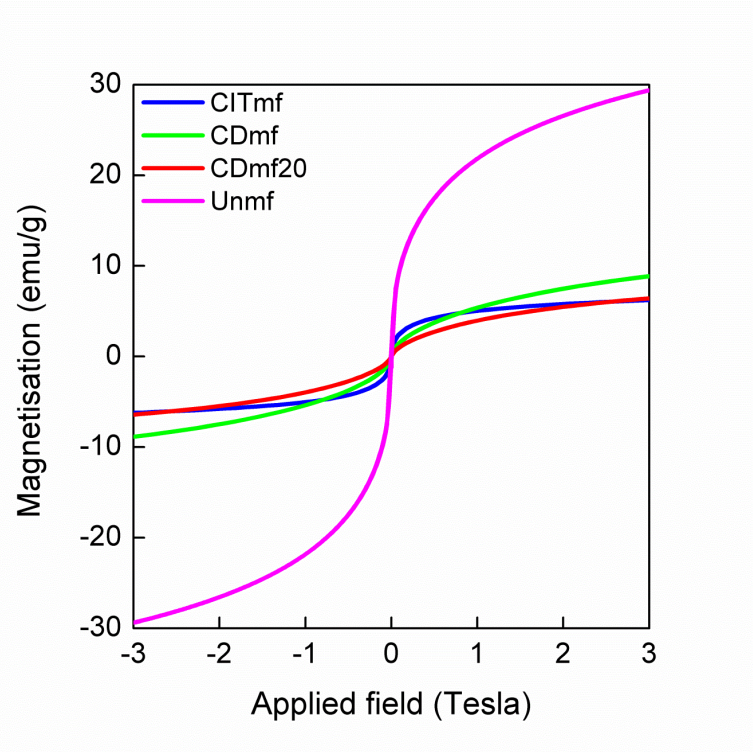

Fig. 4 Magnetization curves of the uncoated and different coated iron oxide nanoparticles, measured at room temperature.

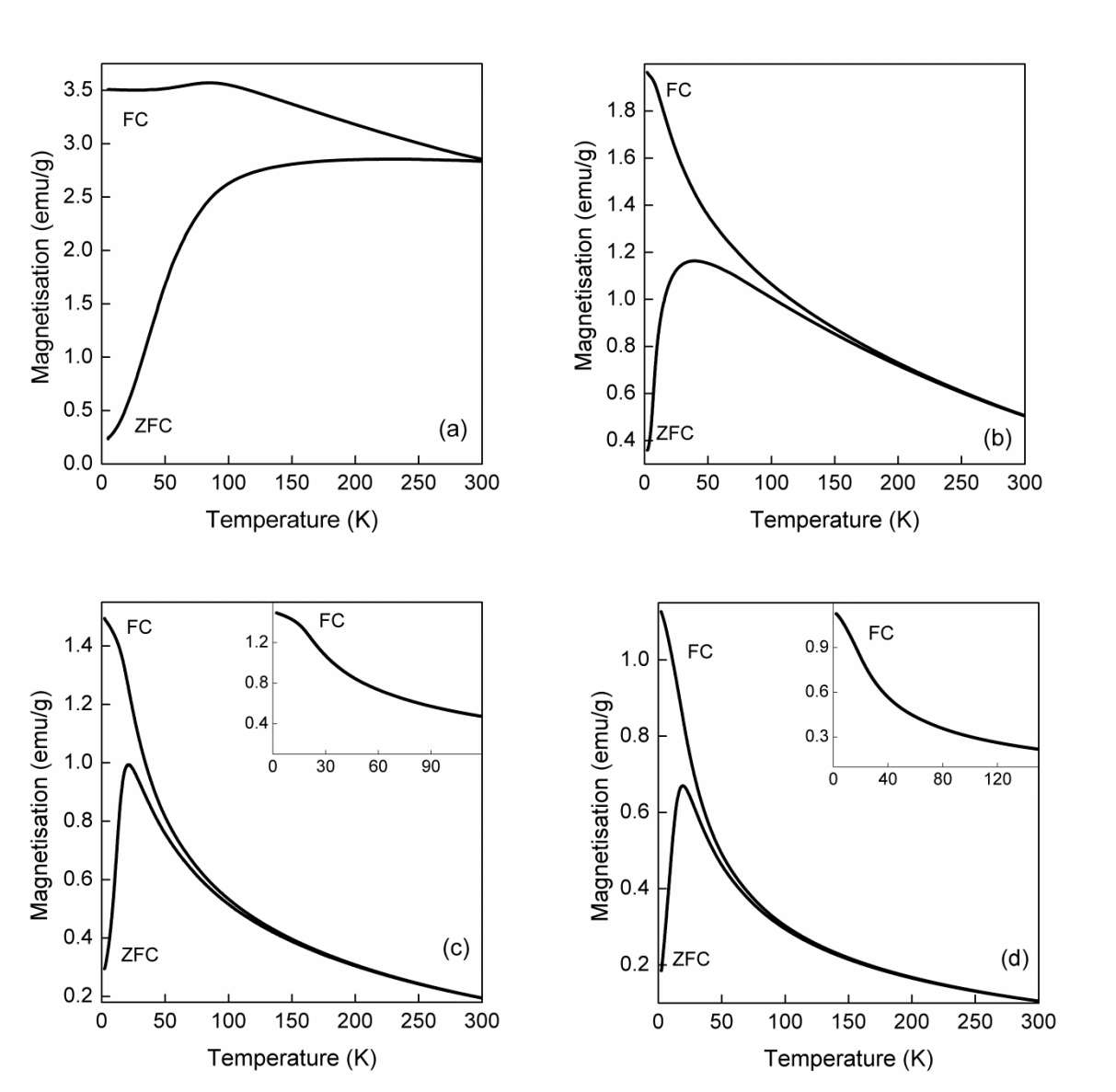

Fig. 5 ZFC and FC magnetization curves of (a) uncoated magnetite nanoparticles (Unmf), (b) CIT coated nanoparticles (CITmf), (c) CD-CIT coated nanoparticles (CDmf), and (d) CUR loaded CDmf nanoparticles(CDmf20), measured in a field of 50 Oe. The insets of (c) and (d) show the enlarged FC curves at low temperatures.

The M vs H curves of the iron oxide samples measured at room temperature, before and after surface modifications, are shown in Fig. 4. The lower values of the magnetization (emu/g of sample) of the surface modified samples are due to the non-magnetic organic molecules present. Continuous increase in the magnetization at higher fields and the absence of magnetic hysteresis

(zero coercivity) confirm that the iron oxide nanoparticles are superparamagnetic. This is further confirmed from temperature dependent magnetization measurements. The zero field cooled (ZFC) and field cooled (FC) magnetization curves of the uncoated and the different coated nanoparticles are compared in Fig. 5. The superparamagnetic blocking temperature (T_B), corresponding to the temperature at which a maximum is observed in the zero field cooled (ZFC) magnetization curve, for the uncoated (Unmf) and citric acid coated (CITmf) samples are obtained as 110 K and 40 K, respectively. Inter-particle magnetic interactions (dipolar and exchange) are known to be reduced or suppressed after coating the magnetic nanoparticles using suitable surfactants due to the decreasing magnetic anisotropy contributed by these interactions and this is evidenced by the decrease in the value of T_B after capping. CDmf and the inclusion complex CDmf20 show almost comparable values of T_B as 20 K. The lower value of T_B for CDmf and CDmf20, compared to the value for CITmf, is due to the further decrease in the anisotropy due to the suppression of magnetic dipolar interactions due to the larger molecules separating the nanoparticles. The FC magnetization of CITmf, CDmf and CDmf20 increases continuously below the blocking temperature which is not observed for Unmf. This behavior shows that the particles are well separated in the case of the coated nanoparticles, where the coatings suppress the magnetic dipolar and exchange interactions between the particles.[36] The FC curve of Cdmf shows a saturating trend at very low temperatures (inset of Fig. 5(c)) whereas this trend is not observed for CDmf20 (inset of Fig. 5(d)). This explains the further suppression of the dipolar interactions due to the increasing separation between the nanoparticles after inclusion of curcumin in the CD cavities.

The possible mode of interaction between the cyclodextrin cavity and curcumin is the encapsulation of the benzene ring of curcumin in the cavity of CD. An inclusion complex is formed by increasing the distance between two magnetite nanoparticles. Based on the results, a schematic representation of the formation of a possible supramolecular self-assembly of the nanoparticles of the curcumin inclusion complex can be represented as shown in Scheme 2. CD is represented as a truncated cone with large and small openings at two ends. The hydroxyl groups are at the two rims of the cone and the interior has hydrocarbon chains, making it hydrophobic. The CH_3 protons interact with the aromatic ring of the curcumin via CH-π interaction.[37]

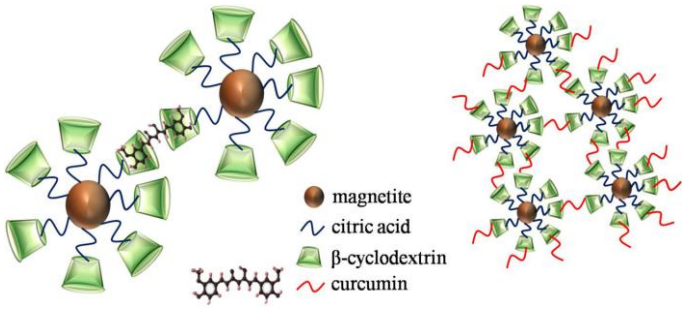

Scheme 2: Mode of binding of modified CD to iron oxide nanoparticles. (A) inclusion complex formed by trapping curcumin in the cyclodextrin cavity and (B) self-assembly of the nanoparticles after inclusion of curcumin.

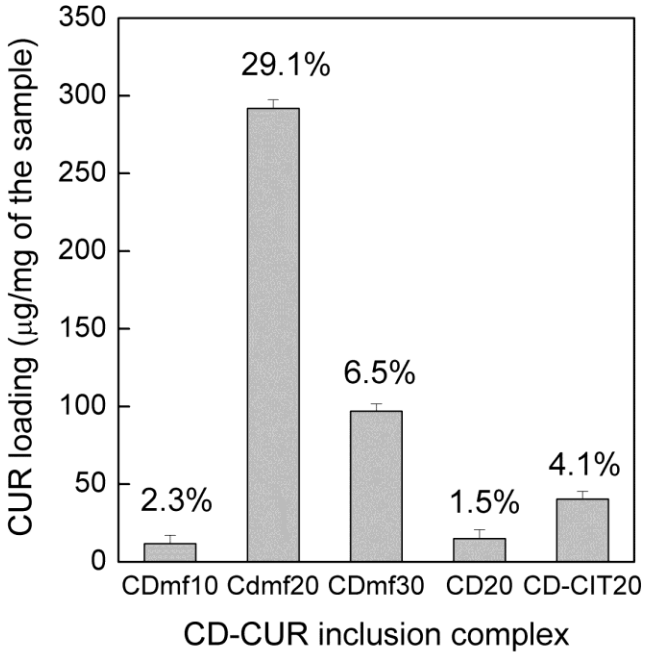

Fig. 6 Graph showing the amount of CUR loaded per mg of the sample (CDmf10, CDmf20 and CDmf30) compared with CUR inclusion complex of bare β-CD (CD20) and CD-CIT (CD-CIT20). The numbers in percentage represent the loading efficiency.

The CD-CIT coated magnetite nanoparticles (CDmf) formed stable water dispersion on re-dispersing the powder obtained from the synthesis procedure described. The CD-CIT coated nanoparticles dispersed in water are treated with curcumin at different weight ratios. The curcumin inclusion complexes, CDmf10, CDmf20 and CDmf30, are analyzed for their curcumin

loading capacity (Fig. 6). The encapsulation efficiency was found to be higher in the case of 1:1 weight ratio of the sample and curcumin (CDmf20) is used (20 g each).The encapsulation efficiency of the coated nanoparticles is also compared with that of bare CD as well as the CD-CIT complex (Fig. 6). Higher efficiency is observed for CD-CIT (4.1%) compared to CD (1.5%). The higher inclusion complexation of CD-CIT (host) to curcumin (guest), compared to that of CD as the host, can be due to the higher solubility CD-CIT due to the binding of the citrate group. The solubility of bare β-cyclodextrin in water is found to be ~18mg/ml, comparable to that reported in the literature,[18] whereas the solubility of CD-CIT complex is obtained as ~60 mg/ml. The curcumin loading efficiency of CDmf is found to be much larger than that obtained by using polymer nanoparticles.[31] Polymeric nanoparticles are studied as a carrier of hydrophobic drugs of which poly(lactic-co-glycolic acid) nanoparticles (PLGA nanoparticles) are the most studied. PLGA nanoparticles show a maximum curcumin loading of about 5–10%.[22,38] The amount of curcumin loaded in the case of CD-CIT bound on magnetite nanoparticles is larger than that of the bare CD-CIT complex. In the case of CD-CIT coated nanoparticles, the cyclodextrin cavities are probably more ordered (see Scheme 2) which results in higher encapsulation efficiency. Hence, the coating of the magnetite nanoparticles with the CD-CIT complex increases the curcumin encapsulation efficiency of β-cyclodextrin. Natural therapeutic agents like curcumin needs to be supplied at a higher dose at the affected site,[28] and hence the enhanced drug loading efficiency on the CD-CIT modified coated nanoparticles may be highly effective for drug delivery applications.

The zeta potential of the different formulations is measured by dispersing them in water. The zeta potential of CDmf is measured as -19.2 mV. CITmf also gave stable water dispersion with a zeta potential of -21.8 mV. The negative zeta potential values help repel the particles in the suspension resulting in long term stability by avoiding aggregation of the particles.[27] The zeta potential for CDmf10, CDmf20 and CDmf30 are obtained as -33.2, -30.3 and -35.8 mV, respectively, indicating the high stability of the dispersions. The relatively lower zeta potential of the highly loaded CDmf20 is due to the blocking of the -OH groups by the curcumin molecule. The negative charge indicates that the unsubstituted -OH groups are pointing towards the aqueous surrounding thereby rendering the hydrophilicity.[25]

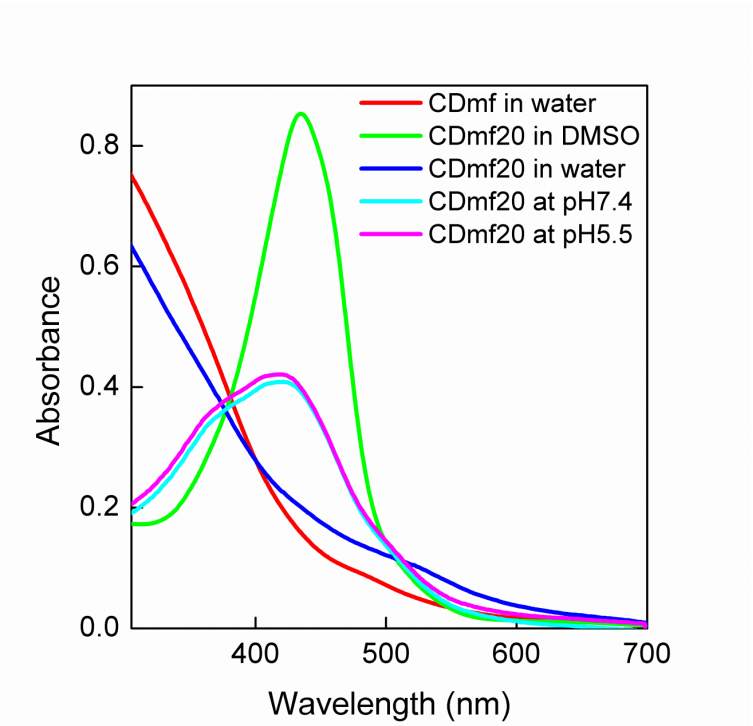

Fig. 7 UV-visible spectra of CD-CIT coated (CDmf) and curcumin loaded (CDmf20) nanoparticles dispersed in water. Spectra of CDmf20 dispersed in DMSO as well as in buffer solutions (pH of 7.4 and 5.5) are also shown which show the distinct peak of curcumin.

The curcumin loaded inclusion complex (CDmf20) did not show the peaks of curcumin in the FT-IR spectra (spectra not shown), especially the peaks of aromatic ring, since the aromatic group is effectively bound inside the cavity of CD. Moreover, it has been reported that the curcumin bands are masked in the IR spectra when CD is present along with curcumin due to the overlapping of the bands of CD and curcumin.[39] Similarly, the UV-visible spectra also do not show any sharp peak at 425 nm which is the characteristic absorption maximum of curcumin. However, the inclusion complex once treated with dimethyl sulfoxide (DMSO) gives the characteristic peak of curcumin, as shown in Fig. 7, where the UV spectra of CDmf dispersed in different media are compared. The UV-Vis spectrum of the magnetic fluid with curcumin loaded in the CD cavity is comparable with that of the nanofluid without curcumin. In aqueous media, the CDmf20 sample with the highest encapsulation efficiency does not show the characteristic peak of CUR whereas once the sample is dispersed in DMSO, the characteristic peak at 425 nm is observed, due to the release of CUR from the CD cavity in the solvent DMSO. The higher

solubility of CUR in DMSO compared to that in water renders CUR to overcome its interaction with the -OH group of the CD cavity.

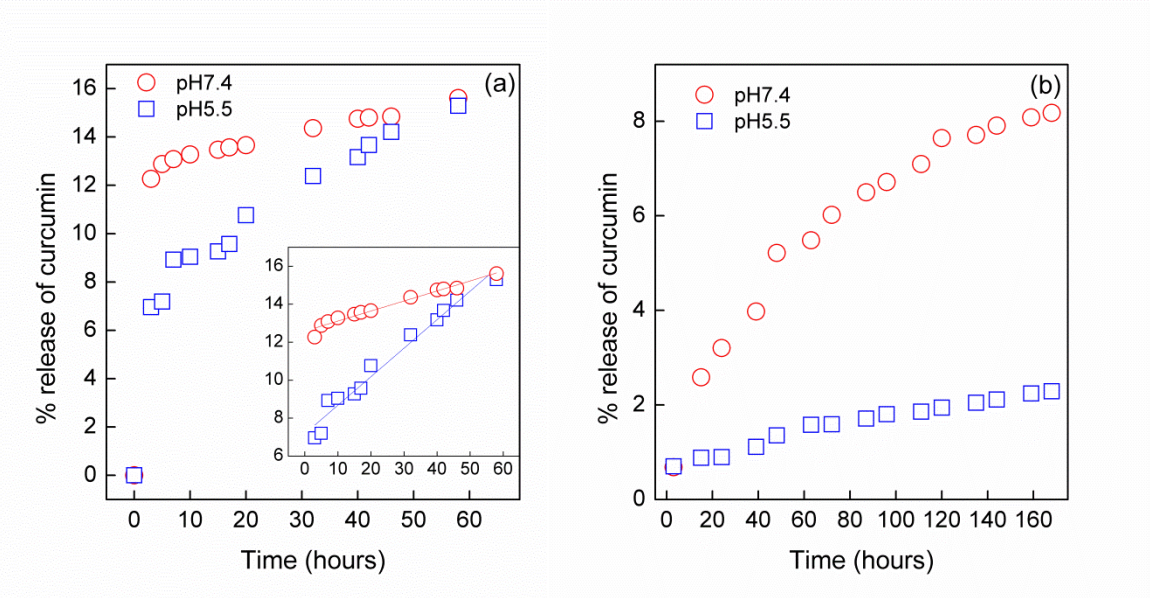

Fig. 8 The drug (curcumin) release profile of (a) CDmf and (b) CURmf at pH7.4 and 5.5. The inset of (a) shows the zero order fitting curves of the release profile.

The release profile of CUR from CDmf20 sample was analyzed at the physiological pH 7.4 and that of the diseased cells pH 5.5, as reported in the literature.[40,41] The release profiles are compared with nanoparticles directly coated with CUR (CURmf). As shown in Fig. 8, the amount of CUR released from the CD cavity is very low at pH 5.5, initially, compared to that released at the physiological pH 7.4. In the case of CDmf there is an initial burst release whereas the curcumin directly coated on the magnetite nanoparticles shows a pulsatile release at the initial stage itself. The amount of curcumin released from CURmf is very low compared to that from CDmf. Stella *et al* have reported the mechanism of drug release from CD cavities, where dissociation being the major release mechanism.[42] The amount of CUR released is plotted against time and fitted to a straight line using the equation

$$Q=Q_0+k_0t$$

where Q is the % release at time t and Q_0 is the % drug released at zero time (always zero) and k_0 is the zero order rate constant.[43] The release profile of CURmf follows the zero order kinetics at both the investigated pH values from the initial time itself whereas the CDmf shows a burst release of CUR followed by constant release. The amount of CUR released from the CDmf sample at a particular time is larger than that compared to CURmf.

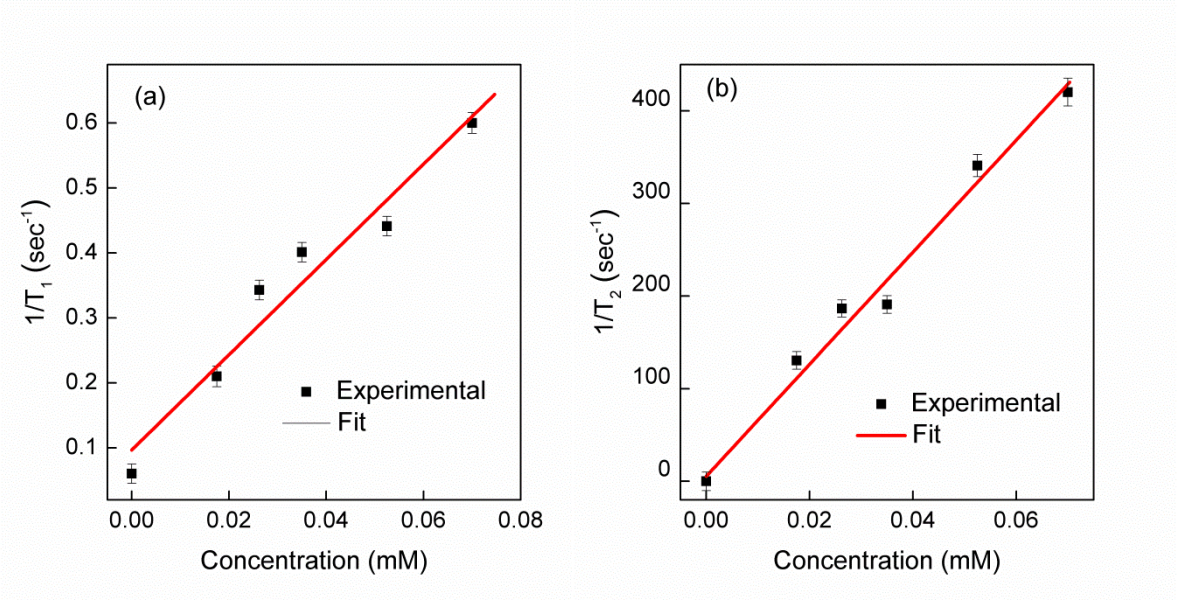

Fig. 9 The reciprocals of (a) spin lattice (T_1) and (b) spin-spin (T_2) relaxation times plotted against concentration.

The relaxivity of cyclodextrin coated magnetite nanoparticles is measured on an NMR spectrophotometer at a magnetic field of 9.4 T and frequency of 400 MHz. The CDmf sample was dispersed in water at different concentrations and the spin-lattice relaxation time T_1 and spin-spin relaxation time T_2 are measured. The reciprocals of the relaxation times are plotted against concentration (Fig. 9) to obtain the corresponding relaxivity values r_1 and r_2 which describe the ability to shorten the relaxation times per millimole of the concentration of contrast agent.[44] The relaxivity values, r_1 and r_2, calculated from the slopes of the plots are 0.0082 $mM^{-1}s^{-1}$ and 6.875 $mM^{-1}s^{-1}$, respectively. The r_2/r_1 ratio is obtained as 838. The r_2 and r_1 values are calculated by considering the particle diameter as 5nm as obtained from TEM, which will have approximately 880 magnetic iron ions.[45] The relaxivity values are known to depend on the

frequency as well as the applied magnetic field and the relaxivity ratio, r_2/r_1, decides whether a material can be used as a contrast agent or not.[46,47] The r_2/r_1 ratio is larger than the minimum threshold (= 2) value required to be used as an effective contrast agent.[48] Hence the modified cyclodextrin coated nanoparticles can be used as a negative contrast agent in MRI, along with the capability of the delivery of curcumin.

IV. Conclusions

Magnetite nanoparticles coated with citrate modified β-cyclodextrin has been synthesized and characterized using TEM, DLS, XRD, FT-IR and UV-visible spectroscopy. The magnetic characteristics are studied using a SQUID-VSM. The cavity of CD on the coated nanoparticles forms an inclusion complex with curcumin and the curcumin loading efficiency is found to be larger than that on free CD. The *in vitro* release profile shows higher amount of CUR release as compared to CUR directly coated on the magnetite nanoparticles. CUR is released in the initial stage at a faster rate known as the "burst release" followed by release at a constant rate following the zero order kinetics at both pH = 7.4 and pH = 5.5. Hence, the as-synthesized nanoparticles, which form a stable fluid in water, can be effectively used for targeting and delivery of hydrophobic drugs to the affected site. The magnetic core adds the benefit of targeting *via* an external magnetic field. The relaxivity of the nanofluid was studied at a frequency of 400 MHz. The calculated relaxivity ratio is well above the minimum threshold value to be used as a negative contrast agent in MRI. Hence, the synthesized nanoparticles which form a stable water suspension can be simultaneously used for imaging, targeting and delivery of hydrophobic drugs to the affected site.

Acknowledgements

K. N. Jayaprabha is grateful to Council of Scientific and Industrial Research (CSIR), India, for financial assistance in the form of a research fellowship.

References

1. W. H. D. Jong and J. P. Borm, *Int. J. Nanomedicine,* 2008, **3**, 133-149.

2. M. Jones and J. C. Leroux, *Eur. J. Pharm. Biopharm.,* 1999, **48**, 101-111.

3. V. P. Torchilin, *J. Control. Release*, 2001, **73**, 137-172.

4. M. Colombo, S. C. Romero, M. F. Casula, L. Gutièrrez, M. P. Morales, I. B. Böhm, J. T. Heverhagen, D. Prosperi and W. J. Parak, *Chem. Soc. Rev.*, 2012, **41**, 4306-4334.

5. S. Kayal and R. V. Ramanujan, *Mater. Sci. Eng., C* 2010, **30**, 484-490.

6. C. Xu and S. Sun, *Adv. Drug Deliv. Rev.*, 2013, **65**, 732-743.

7. M. Liong, J. Lu, M. Kovochich, T. Xia, S. G. Ruehm, A. E. Nel, F. Tamanoi and J. I. Zink, *ACS Nano*, 2008, **2**, 889-896.

8. M. Mahmoudi, S. Sant, B. Wang, S. Laurent and T. Sen, *Adv. Drug Deliv. Rev.*, 2011, **63**, 24-46.

9. Y. J. Wang, *Quan. Imaging Med. Surg.*, 2011, **1**, 35-40.

10. T. K. Jain, J. Richey, M. Strand, D. L. Leslie-Pelecky, C. A. Flask and V. Labhasetwar, *Biomaterials*, 2008, **29**, 4012-4021.

11. S. Laurent, D. Forge, M. Port, A. Roch, C. Robic, L. V. Elst and R. N. Muller, *Chem. Rev.*, 2008, **108**, 2064-2110.

12. A. K. Gupta and M. Gupta, *Biomaterials*, 2005, **26**, 3995-4021.

13. M. Sun, Y. Gao, C. Guo, F. Cao, Z. Song, Y. Xi, A. Yu, A. Li and G. Zhai, *J. Nanopart. Res.*, 2010, **12**, 3111-3122.

14. J. Lu, M. Liong, J. I. Zink and F. Tamanoi, *Small*, 2007, **3**, 1341-1346.

15. K. Uekama, F. Hirayama and T. Irie, *Chem. Rev.*, 1998, **98**, 2045-2076.

16. A. Vyas, S. Saraf and S. Saraf, *J. Incl. Phenom. Macrocycl. Chem.* 2008, **62**, 23-42.

17. F. Hirayama and K.Uekama, *Adv. Drug Deliv. Rev.*, 1999, **36**, 125-141.

18. J. Zhang and P. X. Ma, *Adv. Drug Deliv. Rev.*, 2013, **65**, 1215-1233.

19. M. E. Brewster and T. Loftsson, *Adv. Drug Deliv. Rev.*, 2007, **59**, 645-666.

20. T. K. Biji and R. H. Scofield, *Trends Pharmacol. Sci.*, 2009, **30**, 334-335

21. R. Wilken, M. S. Veena1, M. B. Wang and E. S. Srivatsan, *Mol. Cancer*, 2011, **10**, 12-31.

22. P. Verderio, P. Bonetti, M. Colombo, L. Pandolfi and D. Prosperi, *Biomacromolecules*, 2013, **14**, 672-682.

23. S. S. Banerjee and D. H. Chen, *Chem. Mater.*, 2007, **19**, 6345-6349.

24. M. M. Yallapu, M. Jaggi and S. C. Chauhan, *Macromol. Biosci.*, 2010, **10**, 1141-1151.

25. H. Rachmawati, C. A. Edityaningrum and R. Mauludin, *AAPS Pharm. Sci. Tech.*, 2013,**14**, 1303-1312.

26. V. R. Yadav, S. Suresh, K. Devi and S. Yadav, *AAPS Pharm. Sci. Tech.*, 2009, **10**, 752-762.

27. M. M. Yallapu, S. F. Othman, E. T. Curtis, B. K. Gupta, M. Jaggi and S. C. Chauhan, *Biomaterials*, 2011, **32**, 1890-1905.

28. K. El-Tahlawy, M. A. Gaffar and S. El-Rafie, *Carbohydr. Polym.*, 2006, **63**, 385-392.

29. V. Sreeja, K. N. Jayaprabha and P. A. Joy, *Appl. Nanosci.*, 2014, **DOI** 10.1007/s13204-014-0335-0.

30. K. N. Jayaprabha and P. A. Joy, *J. Nanofluids*, 2014, **3**, 1-7.

31. M. M. Yallapu, M. Jaggi and S. C. Chauhan, *Colloids Surf., B* 2010, **79**, 113-125.

32. N. V. Roik and L. V. Belyakova, *J. Incl. Phenom. Macrocycl. Chem.*, 2011, **69**, 315-319.

33. L. A. C. Cruz, C. A. M. Perez, H. A. M. Romero and P. E. G. Casillas, *J. Alloys Compd.*, 2008, **466**, 330-334.

34. B. D. Cullity and S. R. Stock, *Elements of X-ray diffraction*, Prentice Hall, New Jersey, 3rd edn., 2001.

35. J. Szejtli, *Chem. Rev.*, 1998, **98**, 1743-1753.

36. V. Sreeja and P. A. Joy, *Int. J. Nanotech.*, 2011, **8**, 907-915.

37. R. K. Raju, H. Hillier, N. A. Burton, M. A. Vincent, S. Doudou and R. A. Bryce, *Phys. Chem. Chem. Phys.*, 2010, **12**, 7959-7967.

38. T. Govender, S. Stolnik, M. C. Garnett, L. Illum and S. S. Davis, *J. Control. Release*, 1999, **57**, 171-185.

39. P. R. Krishna Mohan, G. Sreelakshmi, C.V. Muraleedharan and R. Joseph, *Vib. Spectrosc.*, 2012, **62** , 77- 84.

40. Y. Tang, Z. Teng, Y. Liu, Y. Tian, J. Sun, S. Wang, C. Wang, J. Wang and G. Lu, *J. Mater. Chem. B*, 2014, **2**, 4356-4362.

41. L-C. Ho, C-H. Hsu, C-M. Ou, C-W. Wang, T-P. Liu, L-P. Hwang, Y-Y. Lin and H-T. Chang, *Biomaterials*, 2015, **37**, 436-446.

42. V. J. Stella, V. R. Rao, E. A. Zannou and V. Zia, *Adv. Drug Deliv. Rev.*, 1999, **36**, 3-16.

43. S. Dash, P. N. Murty and L. Nath, *Acta Pol. Pharm.*, 2010, **67**, 217-223.

44. U. I. Tromsdorf, O. T. Bruns, S. C. Salmen, U. Beisiegel and H. Weller, *Nano Lett.*, 2009, **9**, 4434-4440.

45. J. Bridot, A. Faure, S. Laurent, C. Rivière, C. Billotey, B. Hiba, M. Janier, V. Josserand, J. Coll, L. V. Elst, R. Muller, S. Roux, P. Perriat and O. Tillement, *J. Am. Chem. Soc.*, 2007, **129**, 5076-5084.

46. Y. Gossuin, S. Disch, Q. L. Vuong, P. Gillis, R. P. Hermann, J.-H. Park and M. J. Sailor, 2010, **5**, 318-322.

47. Gossuin Y., Gillis P., Hocq A., Vuong Q L. and Roch A., *Wiley Interdiscip. Rev. Nanomed. Nanobiotechnol.* 2009, **3**, 299-310.

48. M. F. Casula, P. Floris, C. Innocenti, A. Lascialfari, M. Marinone, M. Corti, R. A. Sperling, W. J. Parak and C. Sangregorio, *Chem. Mater.*, 2010, **22**, 1739-1748.

Graphical abstract

Water dispersible, β-cyclodextrin functionalized, magnetite nanoparticles are shown to be suitable for the delivery of the hydrophobic drug curcumin, with possible multifunctional applications.